Available online at www.sciencedirect.com
ScienceDirect
Ceramics International 37 (2011) 1415–1422
CERAMICS INTERNATIONAL
www.elsevier.com/locate/ceramint

Sintering behavior of nanostructured WC–Co composite

Akshay Kumar, K. Singh, O.P. Pandey *

School of Physics and Materials Science, Thapar University, Patiala 147004, India

Received 3 January 2011; received in revised form 16 January 2011; accepted 18 January 2011
Available online 26 January 2011

Abstract

Sintering of nanocrystalline WC–Co, retaining the nanoscaled grain sizes is a matter of great interest. Many non traditional methods have been used to achieve this goal as the required result has not been achieved using the traditional method of liquid phase sintering. The present study is an attempt to find out the limitations of traditional sintering method and optimize it to get nanocrystalline WC–Co composites. The effect of temperature, time and composition variation has been studied to see the sintering behavior of nanostructured WC–Co composite. Detailed X-ray diffraction (XRD) analysis as well as microstructural examination showed that sintering at 1350 °C for 1 h with 5% binder composition (Co) is a set of critical temperature, time and composition which can provide the required results. The grain growth is through coalescence. At critical conditions the majorities of WC grains are faceted and attains the shape of prismatic and basal facets.
© 2011 Elsevier Ltd and Techna Group S.r.l. All rights reserved.

Keywords: A. Grain growth; A. Sintering; B. Composites; D. Carbides

1. Introduction

Liquid phase sintering of a mixture of WC and Co powders is the traditional method to obtain WC–Co cemented carbides. The composite consist of faceted WC grains embedded in Co rich binder. Cobalt is used primarily to facilitate liquid phase sintering and acts as a matrix, i.e. a cementing phase between WC grains. A uniform distribution of metal phase in a ceramic is beneficial for improved mechanical properties of the composite [1]. The grain sizes of WC and composition of the binder are also the two major factors which are responsible for the mechanical properties of the composite. Typical the grain sizes of WC ranges from submicron levels to a few microns and the WC–Co composites contain 3–30 wt% cobalt [2]. The technological advances for the synthesis of nanosized WC and Co powders raise prospects for superior mechanical properties [3–10]. The superior mechanical properties of nanoscale materials also have been attributed to the nano-sized WC grains and high volume fraction of grain boundaries, which can be explained by the Hall–Petch equation [11]. Nanocrystalline cemented tungsten carbide production however, remains a technological challenge. The coarsening of nanosized particles is an issue that affects the manufacture of bulk nanocrystalline materials. Studies of the grain growth behavior have found that grain growth occurs rapidly during the early stages of sintering. It was observed that the grain size of the composites increased dramatically from their initial nanometer sizes. McCandlish et al. [3] have shown that the WC grain size in a WC–10 wt% Co alloy obtained by sintering nanosized WC–Co powder was 200 nm after 30 s of sintering at 1400 °C, and it became 2000 nm after additional 30 s. Petersson et al. [12] and Porat et al. [13] also provided the experimental evidence of the sintering and grain growth that indicated large amount of grain growth that occurred at 1200 °C while liquid phase was not expected to form until 1280 °C. It was also found by Schubert [14] that grain growth started during heat-up to the temperature, which is attributed to the high degree of ‘‘meta-stability’’ of the powder. Wang et al. [15] studied grain growth and densification behavior during heating up of nanocrystalline WC–Co powder and showed that the original 10 nm grain size has increased almost 90-fold up to 900 nm by 1400 °C. This explosive grain growth occurs almost instantly during heat-up, with no holding time [15]. A similar finding has also been reported on the sintering behavior by many other researchers [16–18,2,19,20]. Agrawal et al. [21] used non-traditional microwave sintering technique and produced uniform and fine microstructures.

* Corresponding author. Tel.: +91 175 2393116; fax: +91 175 2393020.
E-mail address: oppandey@thapar.edu (O.P. Pandey).

0272-8842/$36.00 © 2011 Elsevier Ltd and Techna Group S.r.l. All rights reserved.
doi:10.1016/j.ceramint.2011.01.001

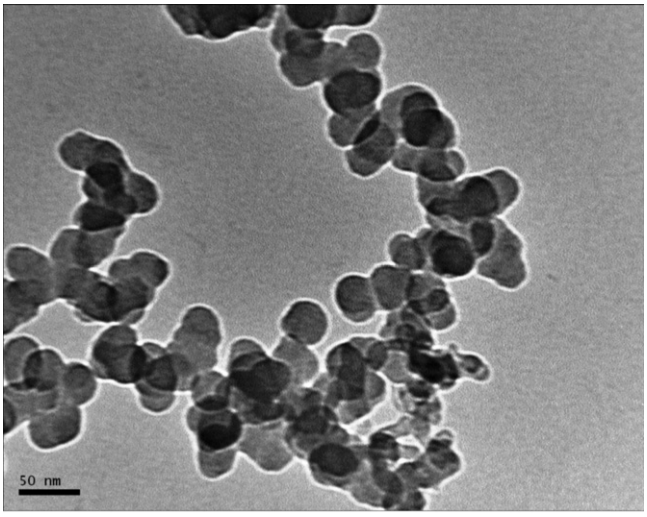

Fig. 1. TEM of WC nano particles.

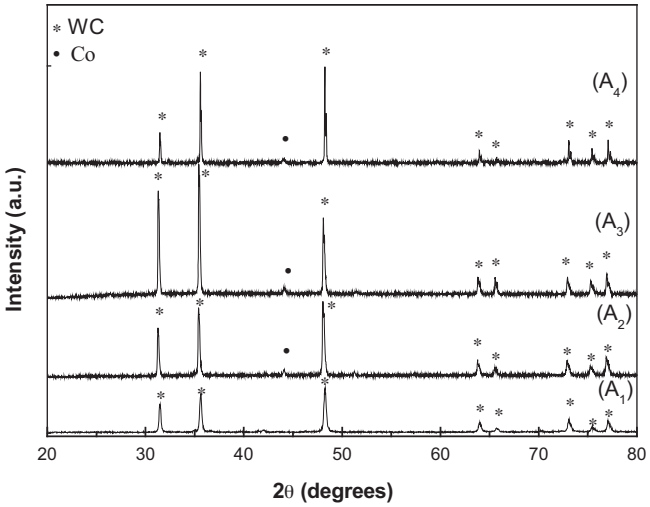

Fig. 2. XRD of samples A_1 to A_4.

Since this technique need optimization, Demirskyi et al. [22] tried to optimize it by studying the neck growth process numerically and comparing it with experimental results.

After this survey, it appears that a critical composition and time exists above which the grain growth accelerates dramatically as a function of temperature which was also proposed by Fang et al. [23]. Moreover, growth of nano WC occurs before sintering takes place [15]. In order to make the material useful for practical applications it is essential to have good bonding between WC and Co particles. If the critical values are known, it may be possible to get a true nanocrystalline WC–Co composite. Our present study is an attempt to find out these critical values. The effect of temperature, sintering time and percentage of cobalt variation on the sintering of nano crystalline WC–Co cemented carbide has been examined in a different way. The particle size and micro strain in the sintered product are related to the microstructure which has been discussed in the text.

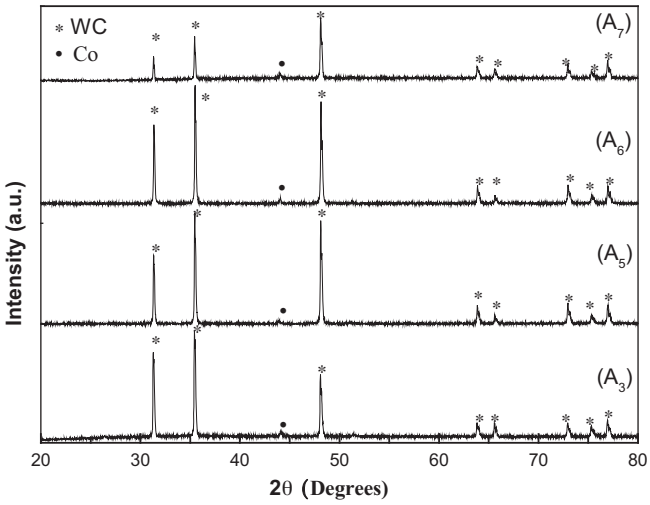

Fig. 3. XRD of samples A_3, A_5 to A_7.

2. Experimental

The preparation of WC nano powders was carried out in a specially designed stainless steel autoclave of 50 ml capacity [9,10]. The TEM micrograph indicates that particle size of synthesized nano WC varies between 30 and 40 nm (Fig. 1). Different composition of WC–Co composites has been prepared by mixing different weight percentage of cobalt nano particles in WC nano particles using FRISCH (Puloerisette) ball mill (Table 1). The dried powder is milled for 4 h

Table 1
Sample label with corresponding sintering temperature, time, composition, particle size (XRD) and micro strain (XRD).

Sample label	Composition wt % (WC/Co)	Sintering time (h)	Sintering temperature (°C)	Particle size (nm) (XRD)	Micro strain (XRD)
A_1	95/5	1	1250	40.41	3.20×10^{-4}
A_2	95/5	1	1300	51.50	6.75×10^{-4}
A_3	95/5	1	1350	66.94	1.54×10^{-4}
A_4	95/5	1	1400	68.14	2.63×10^{-4}
A_5	95/5	2	1350	67.84	2.56×10^{-4}
A_6	95/5	3	1350	70.31	3.75×10^{-4}
A_7	95/5	4	1350	72.64	2.73×10^{-4}
A_8	90/10	1	1350	66.09	7.86×10^{-4}
A_9	85/15	1	1350	66.66	1.90×10^{-4}
A_{10}	80/20	1	1350	66.09	1.54×10^{-4}

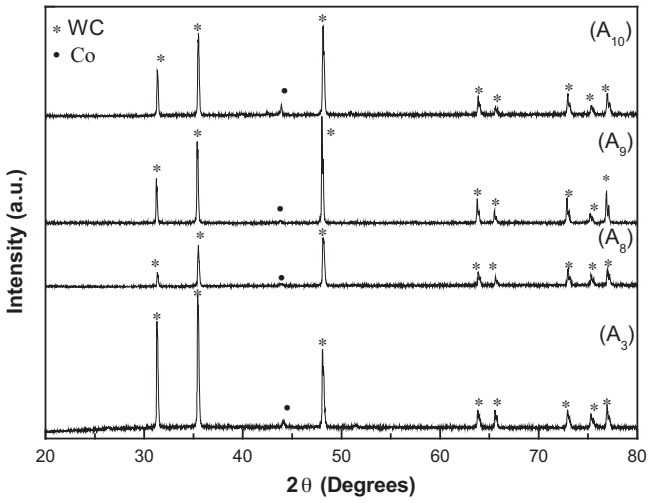

Fig. 4. XRD of samples A_3, A_8 to A_{10}.

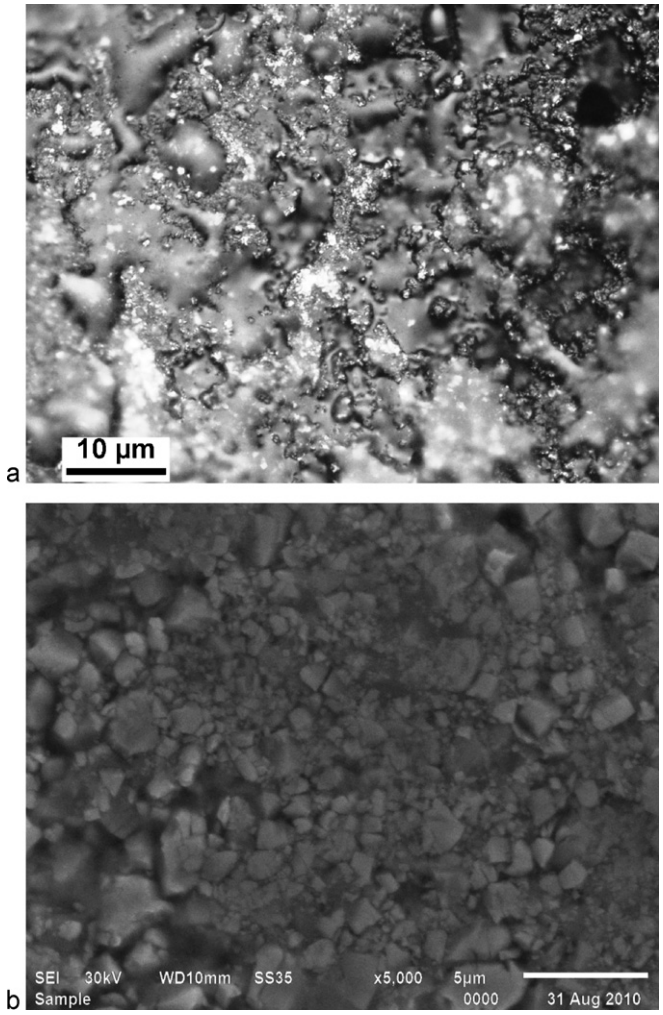

Fig. 5. (a) Optical micrograph of sample A_1. (b) SEM of sample A_1.

using tungsten balls in a tungsten jar at 292 rpm with 1:50 charge to ball ratio. In these mixed powders few drops of 10 mole percent polyvinyl alcohol (PVA) was added. Known weight of dried powders was transferred in a die of 15 mm diameter. The die along with punch was kept below hydraulic press (Polyhedron, India; Model 5010) and a compaction pressure of 503 MPa was applied slowly. After waiting for 1 min, the pressure was released. Afterward the compacted mass was ejected out. The pellets obtained after compaction were sintered at different temperatures for different time in argon atmosphere in a calibrated resistance heating furnace.

2.1. Characterization

All the samples were characterized by X-ray diffraction (XRD) using a Rigaku (Model Geiger flex) X-ray diffractometer using Cu Kα radiation (λ = 1.5418 Å). During the experiment the scanning speed and diffraction angle were 5°/min and 20° to 80° respectively. XRD patterns of the as synthesized composites showed that there is no unwanted phase present. WC and cobalt have not reacted to form complex phases. WC and Cobalt remained unreacted which are indexed with ICDD Card No. 25-1047 and 88-2325 respectively (Figs. 2–4)). It is well established fact that free carbon determines the presence of η phase as well as WC particle

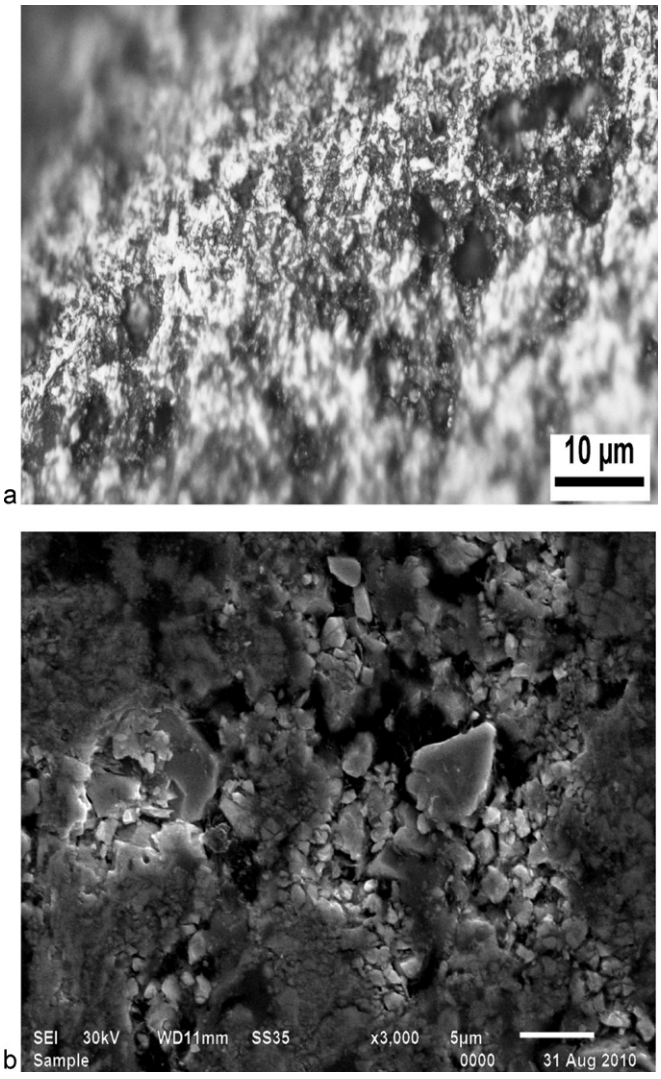

Fig. 6. (a) Optical micrograph of sample A_2. (b) SEM of sample A_2.

shape in a WC–Co alloy [19]. In all the samples no free carbon is present and hence no trace of η phase is there. The broadening in the peaks is related with the size of particles [20].

To determine the crystallite size of the sintered samples, X-ray diffraction line broadening technique was used. As an effect of nano size the crystals are strained and also due to the intense mechanical energy used during composite formation, there inevitably strain energy is stored within the crystal lattice. In order to quantify the grain size accurately by considering the effects of the internal strains, the Stokes and Wilson's formula was used [24]:

$$\beta = \beta_d + \beta_\varepsilon = \frac{0.89\lambda}{d\cos(\theta)} + 4\varepsilon\tan(\theta) \quad (1)$$

where β is full width at half maximum (FWHM) of the diffraction peak after instrument correction; β_d and β_ε are FWHM caused by small grain size and internal strain respectively; and d and ε are, grain size and internal stress or lattice distortion respectively. Experimentally determined line broadening was corrected for $K_{\alpha1}$–$K_{\alpha2}$ separation using the built-in function of the software that was provided with the XRD instrument. The instrumental line broadening was corrected using coarse WC powders (average grain size about 10 μm) as a standard. The instrumental line broadening was subtracted by $\beta^2 = \beta^2_{Exp} - \beta^2_{Instr}$, where β_{Exp} and β_{Instr} are FWHM of the diffraction peak of the experimental profile and instrumental broadening profile respectively [25]. To determine both d and ε from Eq. (1), $(0\,0\,1)_{wc}$, $(1\,0\,0)_{wc}$, $(1\,0\,1)_{wc,}$ $(1\,1\,1)_{wc}$ peaks are used. Grain size and internal strain can be calculated by plotting $\beta\cos(\theta)$ vs. $\sin(\theta)$. The grain size and lattice strain are derived from the intercept and the slope of the linear plot. Microstructural examinations of samples were performed using an optical microscope (Eclipse MA-100, Nikon) and scanning electron microscope (JSM-6510LV (Jeol). For SEM study the sintered pellets were ground and polished. The polished samples were then etched using Morakami's reagent. The details of experimental conditions are given in Table 1. The X-ray diffractogram of sintered samples are given in Figs. 2–4 and microstructures are shown in Figs. 5–14.

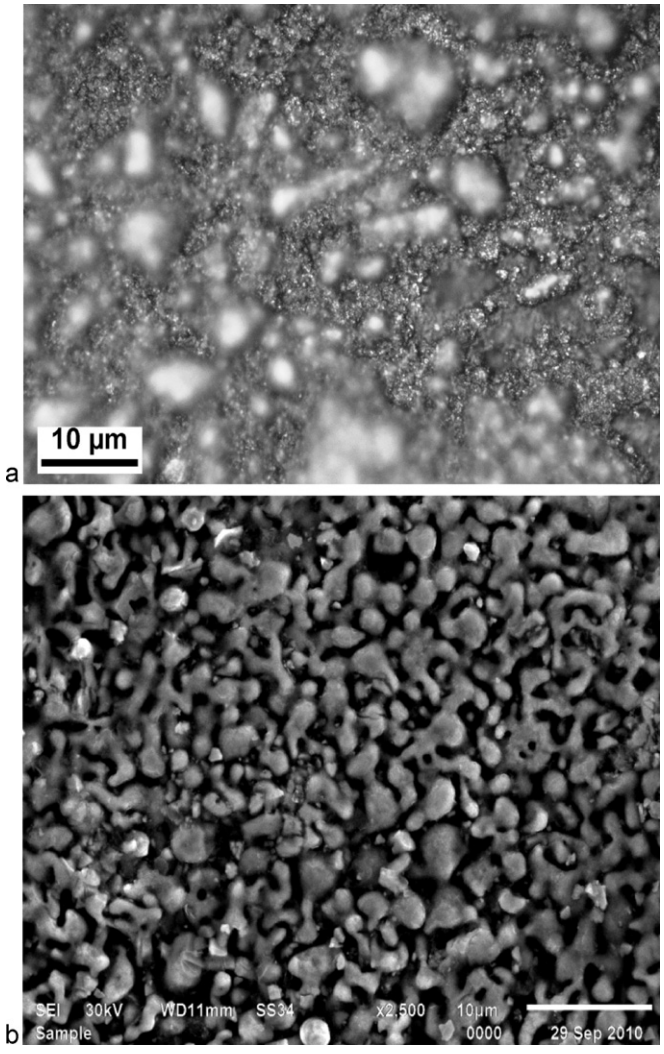

Fig. 7. (a) Optical micrograph of sample A_3. (b) SEM of sample A_3.

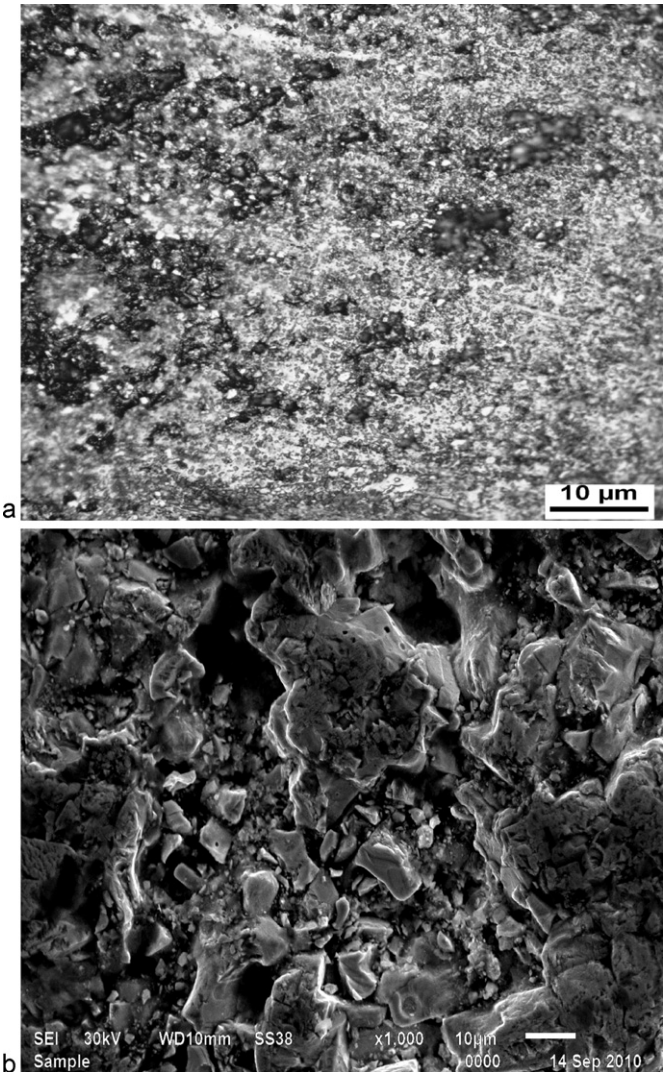

Fig. 8. (a) Optical micrograph of sample A_4. (b) SEM of sample A_4.

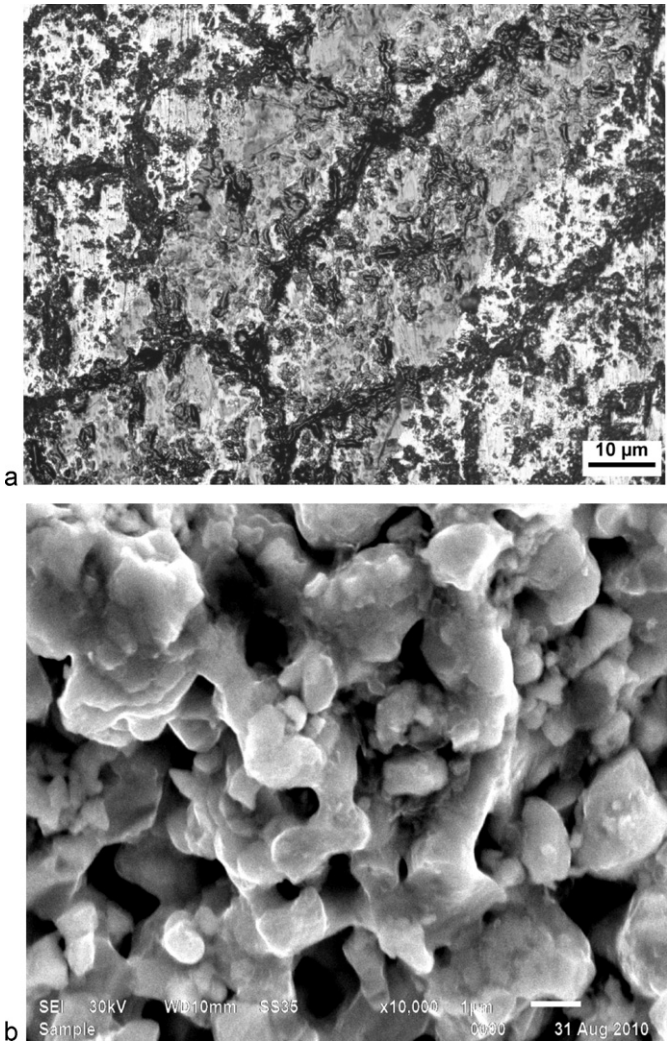

Fig. 9. (a) Optical micrograph of sample A_5. (b) SEM of sample A_5.

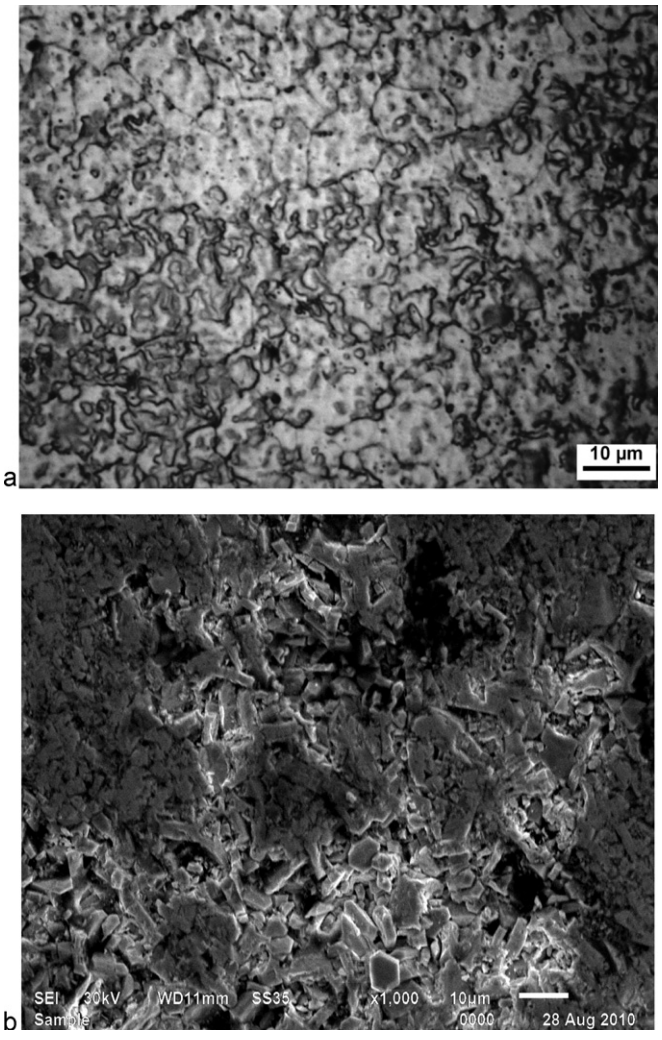

Fig. 10. (a) Optical micrograph of sample A_6. (b) SEM of sample A_6.

3. Results and discussion

3.1. Effect of temperature variation

Green pellets were sintered at different temperatures. The temperature was varied from 1250 °C to 1400 °C with an interval of 50 °C. Sintering time (1 h) and composition (5 wt% cobalt) is kept constant (sample S_1–S_4 in Table 1). XRD analysis of the sintered products showed that no trace of precipitated graphite or the brittle η phases are present [26]. At 1250 °C, particle size of the sintered product varied from 45 nm to 2 μm (Fig. 5(a) and (b)). In this case particle size estimated using XRD line broadening is 40 nm and the material is showing non uniform tensile strain (Table 1). The WC particles did not have any significant changes in grain shape until 1300 °C. Only few isolated WC grains are present in the powder, mainly WC grains agglomerates are observed. The grains do not have a prismatic shape. They are rounded, neither prismatic nor basal facets are observed at the surface of WC grains (Fig. 6(a) and (b)). After the heating stage at 1350 °C for 1 h a significant change in shape of WC grain has taken place. The grains grow through the process of coalescence (Fig. 7(a) and (b)). Furthermore, compared to the samples sintered at 1400 °C for the same time the aggregates that formed during sintering are larger as shown in Fig. 8(a) and (b). The overall analysis of structure indicate that samples containing 5% Co binder have lot of porosity when sintered at 1250 °C and 1300 °C for 1 h ((Figs. 5(a) and (b) and 6(a) and (b)). When the sintering temperature was increased to 1350 °C, homogeneous structure was obtained (Fig. 7(a) and (b)). As the temperature was increased to 1400 °C, material starts flowing causing improper grain growth with porous structure (Fig. 8(a) and (b)). The analysis indicates that 1350 °C sintering temperature is appropriate one to attain uniformly distributed features of WC–Co composite.

3.2. Effect of time variation

In order to see the effect of sintering time the composites were sintered at 1350 °C for 1–4 h at an interval of 1 h. The binder composition (5 wt% cobalt) is kept constant (sample

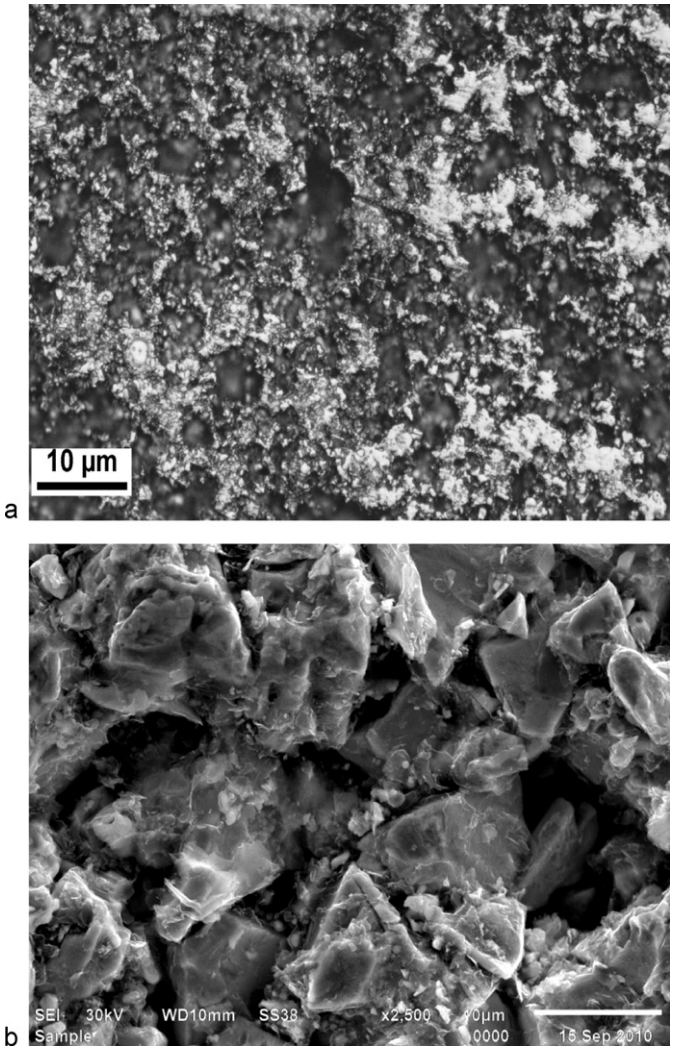

Fig. 11. (a) Optical micrograph of sample A_7. (b) SEM of sample A_7.

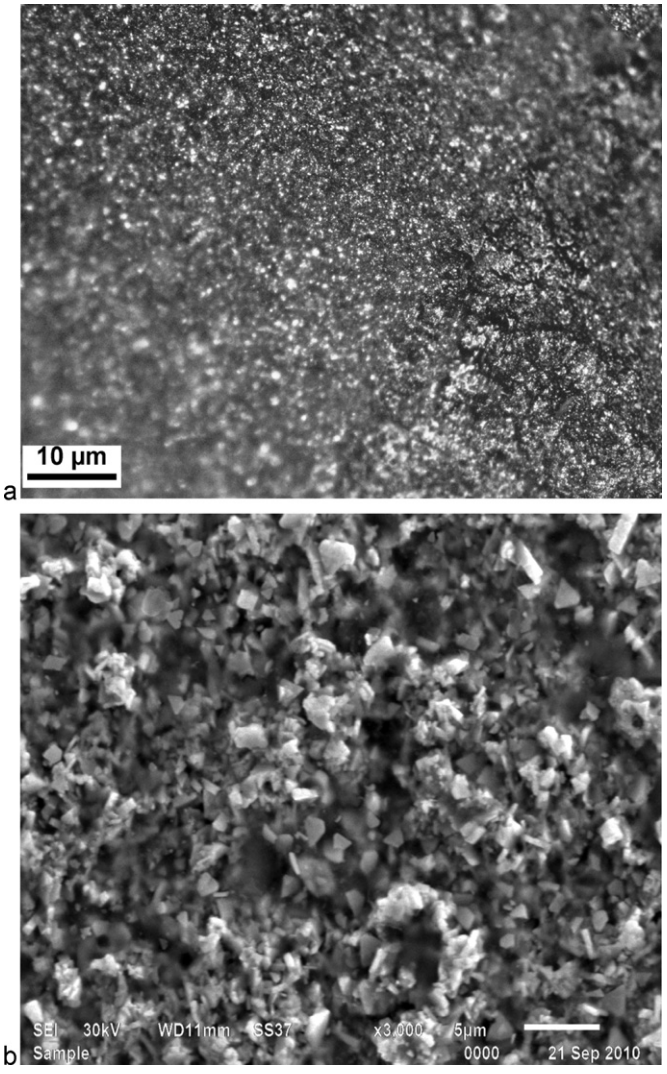

Fig. 12. (a) Optical micrograph of sample A_8. (b) SEM of sample A_8.

A_3, A_5 to A_7 Table 1). The liquid phase sintering started at 1 h heat treatment as can be seen in the flow characteristics in the micrograph (Fig. 7(a) and (b)). The grain size was observed to vary between 0.5 and 4 μm as can be seen in the microstructure (Fig. 7(a) and (b)). The microstructure does not show clear grain boundaries between the layers. However, interconnected continuous flow pattern is observed (black zone). It is logical to reason that there are indeed grain boundaries between the layers because the size of crystallites measured by XRD (66.94 nm) is much smaller than it would be if all these aggregates are individual grains (Table 1). This is a clear evidence of grain growth by coalescence. When the sintering time is increased to 2 h these crystallites starts collapsing and grain growth occurs Fig. 9(a) and (b). Moreover, carbides start forming network structure (Fig. 9(a)) which is not desirable. This may be because of higher volume fraction of WC and higher sintering time. As the heating time is increased further the formation of stable faceted WC particles increases as can be seen in the microstructure (Fig. 10(a) and (b)). Here the network breaks and large particles are formed (Fig. 10(a)). However, this does not lead to a stable one as porosity also exists in the structure (Fig. 10(b)). The overall study indicates that the nano WC particles grow with time. These aggregates disappear and further these are replaced by the angular shaped single crystal grains of larger size that are also like the result of the coalescence (Figs. 9–11(a) and (b)) [2]. The crystallite size showed an increasing trend with the increase in sintering time. It increased to 72.64 nm with the increase in sintering time from 1 to 4 h. The positive slope of $\beta \cos(\theta)$ vs. $\sin(\theta)$ indicates the presence of effective non uniform tensile strain in the crystal lattice which is also verified by the shifting of XRD peaks [27]. Basically 'β' is inversely proportional to the diameter of particle here 'β' of the present sample is comparatively large which corresponds to small diameter of particle [24].

3.3. Effect of composition variation

In order to see the effect of binder (Co), its composition is varied from 5 to 20 wt% in WC–Co composite, with an

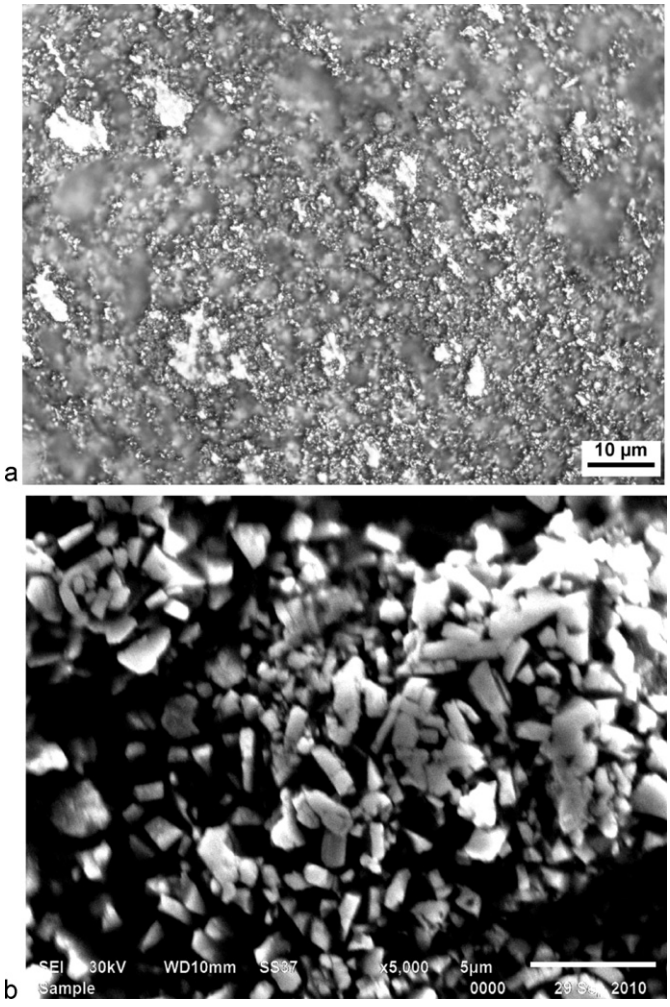

Fig. 13. (a) Optical micrograph of sample A_9. (b) SEM of sample A_9.

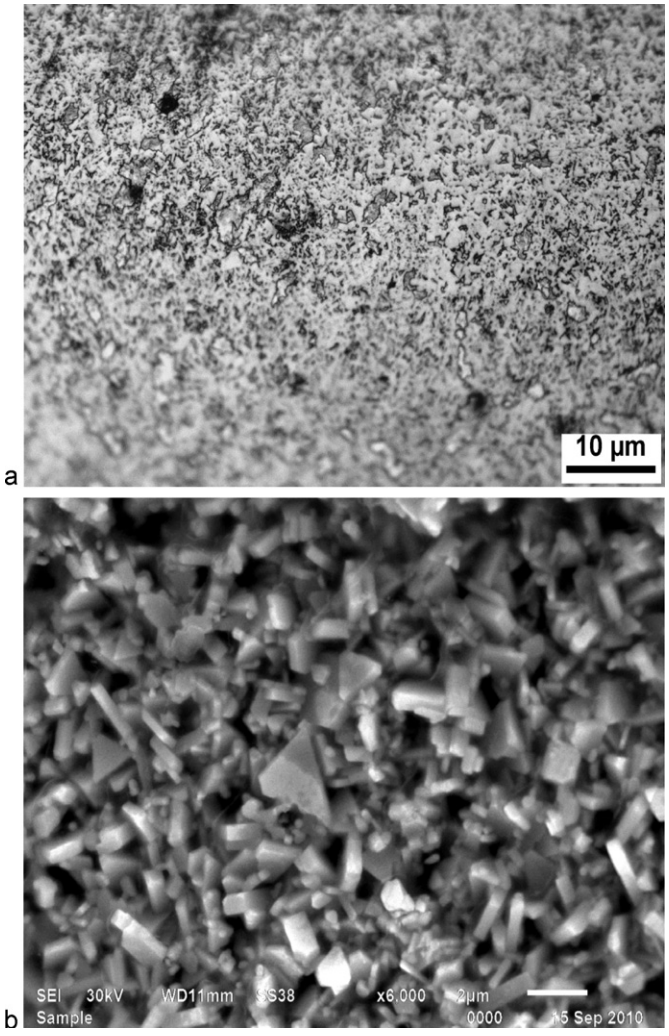

Fig. 14. (a) Optical micrograph of sample A_{10}. (b) SEM of sample A_{10}.

increment of 5 wt%. The heating time and temperature is kept constant (1 h and 1350 °C respectively) as this has shown optimum results. In composite with 5% of cobalt, as discussed earlier the grains grow through the process of coalescence of neighboring grains (Fig. 7(a) and (b)). In composite with 10% of cobalt, microstructure belongs to a two-phase region consisting of WC, and β-Co. Here, the β-Co phase is a cobalt-rich solid solution containing W and C, which is a liquid phase at the sintering temperature (Fig. 12(a) and (b)). When the Cobalt is increased to 15% and 20%, large WC grains are randomly dispersed in the fine grain matrix. The large grains in these composites show similar shapes. WC grains tend to show an elongated rectangular shape (faceted). The majority of WC grains is faceted and accordingly attains the shape of prismatic and basal facets. This means that the WC grains grow preferentially along the [1 0 0] crystal direction together with increase in the Co content of WC–Co composite (Figs. 13 and 14(a) and (b)) [19]. Aggregation of individual platelet crystals along certain preferred orientations resulted in such type of morphology, the grain growth is not by coarsening which would yield smooth and continuous surfaces. The particle size calculated using XRD showed that there is negligible variation in particle size with composition variation, the composite showing non uniform tensile strain (Table 1). The effect of cobalt is logically related to the solubility of W and C in the cobalt phase. The exact mechanism by which cobalt promotes grain growth, however, is worthy of exploring in light of the need to understand the processes of grain growth. Based on the theories of activated sintering [28], cobalt metal that coats WC grains during milling may serve as a conduit for W and C diffusion which results in densification as well as grain growth.

4. Conclusion

The traditional liquid phase sintering can be used for the sintering of nanocrystalline WC–Co. Sintering of WC–Co composites in argon atmosphere does not show any unwanted phase (η). Sintering temperature at 1350 °C is the critical temperature above which the grain growth increased abruptly. The grains grow through the process of coalescence. The majorities of WC grains are faceted and accordingly attain the shape of prismatic and basal facets. The effect of composition is negligible when sintered at critical temperature. The time factor played a vital role, it can be concluded that nano composite

required very less sintering time as compared to conventional micro composites. It is very difficult to control the coarsening of WC grains.

Acknowledgements

The authors are thankful to Council of Scientific and Industrial Research (CSIR) India and Department of Science and Technology, New Delhi for financial assistance.

References

[1] P. Schwartzkopf, R. Kiefer, Cemented Carbides, The Macmillan Company, NY, 1960, pp. 1–13, 55–96.
[2] X. Wang, Z.Z. Fang, H.Y. Sohn, Grain growth during the early stage of sintering of nanosized WC–Co powder, Int. J. Refract. Met. Hard Mater. 26 (2008) 232–241.
[3] L.E. McCandlish, B.H. Kear, B.K. Kim, Processing and properties of nanostructured WC–Co, Nanostruct. Mater. 1 (2) (1992) 119–124.
[4] J. He, M. Ice, S. Dallek, E. Lavernia, Synthesis of nanostructured WC–12 wt% Co coating using mechanical milling and high velocity oxygen fuel thermal spraying, Metall. Trans. A 31A (2) (2000) 541–553.
[5] J.C. Kim, B.K. Kim, Synthesis of nanosized tungsten carbide powder by the chemical vapor condensation process, Scripta Mater. 501 (7) (2004) 969–972.
[6] L. Fu, L.H. Cao, Y.S. Fan, Two-step synthesis of nanostructured tungsten carbide-cobalt powders, Scripta Mater. 44 (7) (2001) 1061–1068.
[7] Z.G. Ban, L.L. Shaw, Synthesis and processing of nanostructured WC–Co materials, J. Mater. Sci. 37 (16) (2002) 3397–3403.
[8] F.L. Zhang, C.Y. Wang, M. Zhu, Nanostructured WC/Co composite powder prepared by high energy ball milling, Scripta Mater. 49 (11) (2003) 1123–1128.
[9] A. Kumar, K. Singh, O.P. Pandey, Reduction of WO3 to nano-WC by thermo-chemical reaction route, Physica E 41 (2009) 677–684.
[10] A. Kumar, K. Singh, O.P. Pandey, Optimization of processing parameters for the synthesis of tungsten carbide (WC) nanoparticles through solvo thermal route, Physica E 42 (2010) 2477–2483.
[11] H. Gleiter, Nanocrystalline materials, Prog. Mater. Sci. 33 (1989) 223–315.
[12] A. Petersson, J. Agren, Rearrangement and pore size evolution during WC–Co sintering below the eutectic temperature, Acta Mater. 53 (6) (2005) 1673–1683.
[13] R. Porat, S. Berger, A. Rosen, Dilatometric study of the sintering mechanism of nanocrystalline cemented carbides, Nanostruct. Mater. 7 (4) (1996) 429–436.
[14] W.D. Schubert, 2000 International Conference on Tungsten Hard Metals and Refractory Alloys, Annapolis, MD, USA, 2000.
[15] X. Wang, Z.Z. Fang, H.Y. Sohn, Grain growth during the early stage of sintering of nanosized WC–Co powder, Int. J. Refract. Met. Hard Mater. 26 (3) (2008) 232–241.
[16] Z.J. Shen, H. Peng, J. Liu, M. Nygren, Conversion from nano- to micron-sized structures: experimental observations, J. Eur. Ceram. Soc. 24 (12) (2004) 3447–3452.
[17] Z. Fang, J.W. Eason, Study of nanostructured WC–Co composites, Int. J. Refract. Met. Hard Mater. 13 (5) (1995) 297–303.
[18] Z. Fang, P. Maheshwari, X. Wang, H.Y. Sohn, A. Griffo, R. Riley, An experimental study of the sintering of nanocrystalline WC–Co powders, Int. J. Refract. Met. Hard Mater. 23 (4–6) (2005) 249–257.
[19] S. Kim, S.H. Han, J.K. Park, H.E. Kim, Variation of WC grain shape with carbon content in the WC–Co alloys during liquid-phase sintering, Scripta Mater. 48 (2003) 635–639.
[20] S.B. Qadri, E.F. Skelton, D. Hsu, A.D. Dinsmore, J. Yang, H.F. Gray, et al., Size-induced transition-temperature reduction in nanoparticles of ZnS, Phys. Rev. B 60 (13) (1999) 9191–9193.
[21] D. Agrawal, J. Cheng, P. Seegopaul, L. Gao, Grain growth control in microwave sintering of ultrafine WC–Co composite powder compacts, in: Proc. Euro PM'99 Conf (Held in Turin Italy, Nov. 1999), 1999, 151–158.
[22] D. Demirskyi, A. Ragulya, D. Agrawal, Initial stage sintering of binderless tungsten carbide powder under microwave radiation, Ceram. Int. 37 (2011) 505–512.
[23] Z. Zak Fang, X. Wang, T. Ryu, K.S. Hwang, H.Y. Sohn, Synthesis, sintering, and mechanical properties of nanocrystalline cemented tungsten carbide – a review, Int. J. Refract. Met. Hard Mater. 27 (2009) 288–299.
[24] G.K. Williamson, W.H. Hall, X-ray line broadening from filled aluminum and wolfram, Acta Metall. 1 (1953) 22–31.
[25] H.H. Tian, M. Atzmon, Comparison of X-ray analysis methods used to determine the grain size and strain in nanocrystalline materials, Philos. Mag. A 79 (8) (1999) 1769–1786.
[26] K.-M. Tsai, C.-Y. Hsieh, H.-H. Lu, Sintering of binderless tungsten carbide, Ceram. Int. 36 (2) (2010) 689–692.
[27] N.S. Ramgir, Y.K. Hwang, I.S. Mulla, J.-S. Chang, Effect of particle size and strain in nanocrystalline SnO_2 according to doping concentration of ruthenium, Solid State Sci. 8 (2006) 359–362.
[28] R.M. German, Quantitative theory of diffusional activated sintering, Sci. Sintering 15 (1) (1983) 27–42.